

Conduction-electron Zeeman splitting in the noble metals

O. Eriksson

Condensed Matter Theory Group, Department of Physics, Uppsala University, P.O. Box 534, S-751 21 Uppsala, Sweden

H. Ohlsén

Swedish Institute of Microelectronics, P.O. Box 1084, S-164 21 Kista, Sweden

J. L. Calais

Department of Quantum Chemistry, Uppsala University, P.O. Box 518, S-751 20 Uppsala, Sweden

(Received 24 April 1989)

Extremal cross-section areas, cyclotron effective masses, and cyclotron-orbit g factors (g_c) have been calculated for three noble metals (copper, silver, and gold) using the relativistic linear muffin-tin orbital (LMTO) method with a Hamiltonian which includes an applied magnetic field. The calculations are compared with experimental results from de Haas-van Alphen measurements performed by other authors. The overall resemblance between theory and experiment shows that the major source of the deviation from the free-electron g value in the noble metals can be explained by spin-orbit interaction. The large difference between calculated and experimentally determined g_c factors found for the neck orbit in gold is discussed.

I. INTRODUCTION

The conduction-electron g factor, describing the Zeeman splitting of opposite-spin Landau levels in a magnetic field, has proven feasible to study over the Fermi surface in metals and alloys using the de Haas-van Alphen (dHvA) effect by techniques such as absolute amplitude measurements, harmonic ratio measurements, and spin-splitting-zero measurements (see, e.g., Refs. 1-4). The dHvA effect reveals the g factor for a single cyclotron orbit (g_c) averaged over the contributing Bloch states at the Fermi energy. In the theoretical expression for the amplitude of the dHvA signal, derived by Lifshitz and Kosevich⁵ (LK), there is a cosine function, called the spin-splitting factor, with the argument

$$r\pi R^* = r\pi E_Z / E_L = r\pi g_c^* m_c^* / 2, \quad (1)$$

where r is the harmonic number of the signal, E_Z is the cyclotron-averaged Zeeman splitting, E_L is the Landau-level energy spacing, and m_c is the cyclotron effective mass expressed in free-electron units. (Henceforward an asterisk is used to distinguish between experimentally and theoretically determined quantities.) Whenever $rR^* = n + \frac{1}{2}$ (where n is an integer) the spin-splitting factor is equal to zero and the dHvA signal for this specific harmonic will vanish. This absence of amplitude is called a spin-splitting zero (SSZ) and can be found as contours of constant rR^* over a Fermi-surface sheet. The mapping out of SSZ contours is the most straightforward method to study the variation of the g_c factor but in order to achieve a full picture of its anisotropy complementary methods are needed, such as the absolute amplitude and/or harmonic-ratio method. In the former technique the ratio between the calculated LK amplitude will give the variation of $\cos(r\pi R^*)$ and in the latter it is possible

to normalize the value of the fundamental amplitude since the cosine factor equals $1/\sqrt{2}$ whenever the second harmonic has an SSZ. The dHvA measurements thus reveal the parameter R^* as a function of angle. With the knowledge of m_c^* , from measurements of the dHvA amplitude as a function of temperature, it is therefore possible to obtain the variation of g_c^* . When comparing effective masses from band-structure calculations and dHvA measurements this is normally done by

$$m_c^* = (1 + \lambda) m_c, \quad (2)$$

where λ is ascribed to the electron-phonon coupling. The g_c^* factor is enlarged by a cyclotron Stoner enhancement⁶ (S_c) and since R^* is, in the same way as the magnetization, not affected by electron-phonon interaction, the cyclotron orbit g factor may be written as

$$g_c^* = S_c g_c / (1 + \lambda) \quad (3)$$

for comparison to theoretical values under the condition that experimentally determined m_c^* values are used when deducing the g_c^* factor. Since the g_c^* factor appears in a cosine function it is in general not possible to determine its absolute value but the dHvA effect offers a unique possibility to measure its anisotropy.

In a recent study, calculations of the conduction-electron Zeeman splitting in the fcc platinum-group metals (rhodium, palladium, iridium, and platinum) are compared to measurements of the g_c^* factor using the dHvA effect (see Ref. 7 and references therein). Both calculations and measurements show an anisotropic behavior of the cyclotron-orbit g factor on parts of the Fermi surface which these metals have in common, namely the Γ -centered (Γ_6) electron sheet and the X -centered hole pockets (X_4) in palladium and platinum. In contrast to

this anisotropy stands the isotropic behavior of the g_c factor on the α orbit centered around the W point on the open-hole sheet in palladium and platinum. This agreement between experiment and calculations involving spin-orbit coupling indicates that the latter is a major source of the behavior of the Zeeman splitting in these metals.

The noble metals constitute an obvious continuation in a comparison of the Zeeman splitting between theory and experiment. Their electronic structures have been, by a large margin, the most extensively studied, both experimentally and theoretically. Due to the large electron-electron exchange enhancement in the transition metals giving rise to a bulk Stoner enhancement factor as high as 8 for palladium and together with a rather large electron-phonon coupling, this complicates the comparison of the g_c factor between calculations and experiment since absolute values are not obtainable from dHvA measurements. However, the noble metals have an electron-phonon enhancement $(1+\lambda)$ and bulk Stoner enhancement factor close to unity which makes a direct comparison possible between theory and experiment, regarding the cyclotron-orbit g factor.

II. THEORY AND METHOD OF CALCULATION

To calculate the g_c factor in the noble metals the linear muffin-tin orbitals (LMTO) method in the atomic-sphere approximation was used. The routine was constructed utilizing the equations given by Skriver⁸ for the Hamiltonian and overlap matrices. To the Hamiltonian the spin-orbit interaction and an applied magnetic field were added. To calculate the lattice sums appearing in the structure constants the technique outlined by Nijboer and de Wette⁹ was used. Only s , p , and d orbitals were included. The code was set up in such a way that the structure constants were calculated for each given \mathbf{k} point, then the Hamiltonian and the overlap matrices and finally the eigenvalues for that specific \mathbf{k} were extracted. The potential parameters, spin-orbit coupling parameters, and Fermi energy used for the noble metals in the constructed routine were obtained from self-consistent LMTO calculations including spin-orbit coupling with a mesh of 505 \mathbf{k} points using the FORTRAN routine package written by Skriver and described in Ref. 8 (for further details see Ref. 7).

When a magnetic field is applied, only Bloch states on extremal areas with \mathbf{k} perpendicular to the magnetic field direction contribute to the cyclotron orbit under study. For such a direction in the crystal coordinate system (θ, ϕ) and for a specific origin the length of the \mathbf{k} vector was changed until the Fermi energy was attained within an accuracy of 0.05 mRy and thus giving $\mathbf{k}_F(\theta, \phi)$. This procedure was carried out with $B=0$ T giving doubly degenerative energy levels, but as the \mathbf{k}_F vector was found, a new calculation was performed with $B=10$ T, thus splitting the degeneracy into E^+ and E^- levels. The local g factor exhibits a tensor nature and may, at the point \mathbf{k}_F and for a specific magnetic field direction $\hat{\mathbf{B}}$, be defined as

$$g(\mathbf{k}_F, \hat{\mathbf{B}}) = (E^+ - E^-) / \mu_B B. \quad (4)$$

The g_c factor can be related to the local g factors contributing to a cyclotron orbit through a time-weighted average¹⁰

$$g_c = \frac{\int_0^{2\pi} |\mathbf{k}_F| g(\mathbf{k}_F, \hat{\mathbf{B}}) (\hat{\mathbf{k}}_F \cdot \mathbf{v}_\perp)^{-1} d\phi'}{\int_0^{2\pi} |\mathbf{k}_F| (\hat{\mathbf{k}}_F \cdot \mathbf{v}_\perp)^{-1} d\phi'}, \quad (5)$$

where the integration is performed around the cyclotron orbit and \mathbf{v}_\perp is the component of

$$\mathbf{v} = \frac{(\nabla_{\mathbf{k}} E)_{\mathbf{k}_F}}{\hbar}$$

in the plane perpendicular to \mathbf{B} . The denominator in Eq. (4) is equal to $2\pi m_c / \hbar$ expressed in the free-electron mass.

The extremal cross-sectional area A perpendicular to the magnetic field is related to the dHvA frequency F through the Onsager relation $F = \hbar A / 2\pi e$ and was calculated from

$$A = \frac{1}{2} \int_0^{2\pi} |\mathbf{k}_F|^2 d\phi'. \quad (6)$$

The calculations of the g_c factor, m_c , and A using Eqs. (4) and (5) were performed by integrating along the cyclotron orbit on the Fermi surface with the Simpson integration technique and $d\phi' = 2.5^\circ$. \mathbf{v}_\perp was calculated using

$$\mathbf{v}_\perp = \frac{E(\mathbf{k}_F + \Delta\mathbf{k}) - E(\mathbf{k}_F - \Delta\mathbf{k})}{2\Delta k} \quad (7)$$

with $\Delta k = 10^{-3} \times 2\pi/a$, where a is the lattice constant.

III. RESULTS

In Figs. 1 and 2 the calculated extremal areas for different cyclotron orbits as a function of magnetic field direction in the symmetry planes are presented. The calculated orbital areas for the rosette (R), the dog bone (D), and the belly (B) are shown in Fig. 1 while the areas for the neck orbit (N) are presented in Fig. 2. The Fermi surface of the noble metals contacts the Brillouin zone boundary in the [111] direction on the otherwise rather spherically shaped surface. This leads to open belly orbit for angles of the magnetic field in the vicinity of 35.3° in the (110) plane and at [110] since these directions represent a cyclotron orbit that passes over two and four [111] directions, respectively. When comparing these results to high-precision dHvA measurements by Coleridge and Templeton¹¹ performed for the same orbits in the symmetry directions, the differences are smaller than 5% for all orbits except for the rosette in copper (8%) and the neck orbits; copper (13%), silver (29%), and gold (8%). The general feature of larger extremal areas for copper than for silver and gold which have similar area size, excluding the neck orbit, is well described by the calculations.

The calculated cyclotron effective masses for the same orbits as presented in Figs. 1 and 2 are shown in Figs. 3(a), 3(b), and 3(c) for copper, silver, and gold, respectively. Experimentally determined masses are shown for

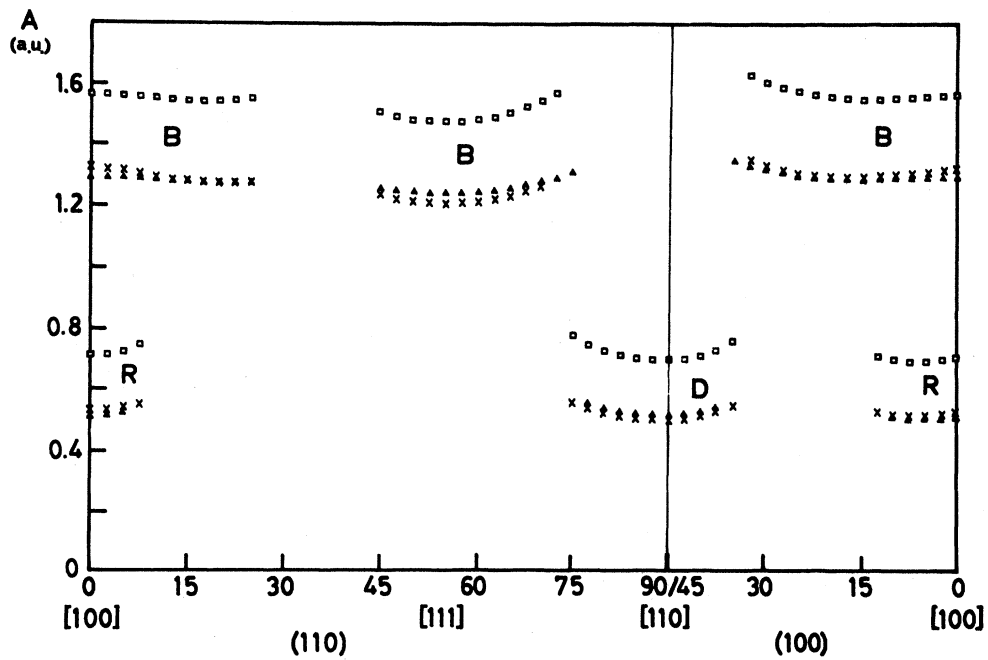


FIG. 1. The cyclotron extremal areas in atomic units as a function of magnetic field direction in the symmetry planes for the belly (*B*), rosette (*R*), and dog-bone (*D*) orbits in copper (\square), silver (\triangle), and gold (\times).

comparison and these were taken from Refs. 12–14 for copper, Refs. 12, 14, and 15 for silver, and Res. 3, 12, 14, and 16 for gold. For the clarity of the figures the same symbols are used for all the experimental data irrespective of what reference to which the data belong. In these figures it can be seen that there is an excellent agreement

between the calculated and experimental values for different angles and orbits. Not including the neck orbit the difference is of the order of, or smaller than, 5% for the three metals, leading to the conclusion that the electron-phonon coupling for these orbits is very small. Regarding the neck orbit the differences are larger result-

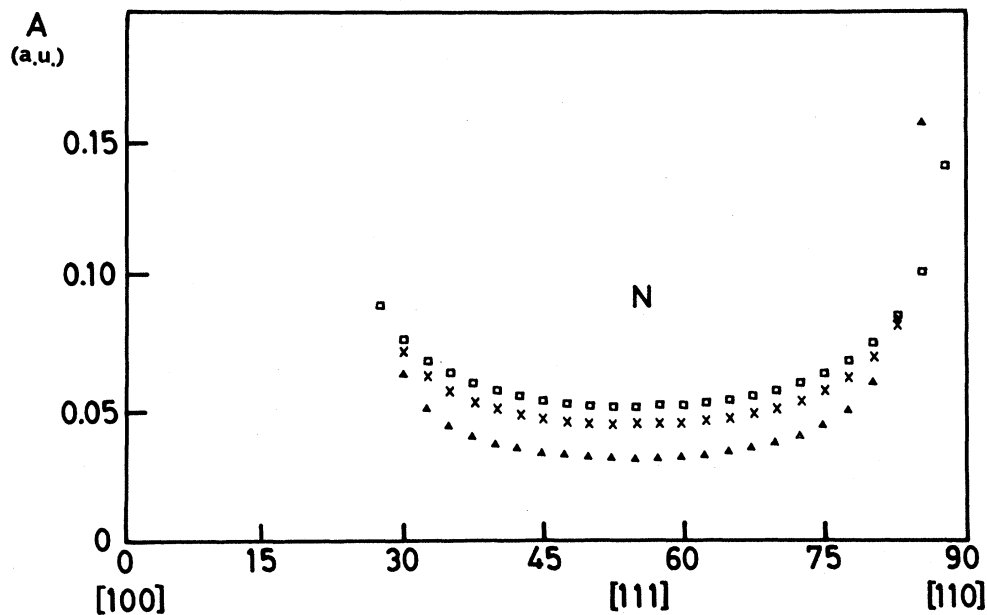


FIG. 2. The cyclotron extremal areas in atomic units as a function of magnetic field direction for the neck orbit (*N*) in copper (\square), silver (\triangle), and gold (\times).

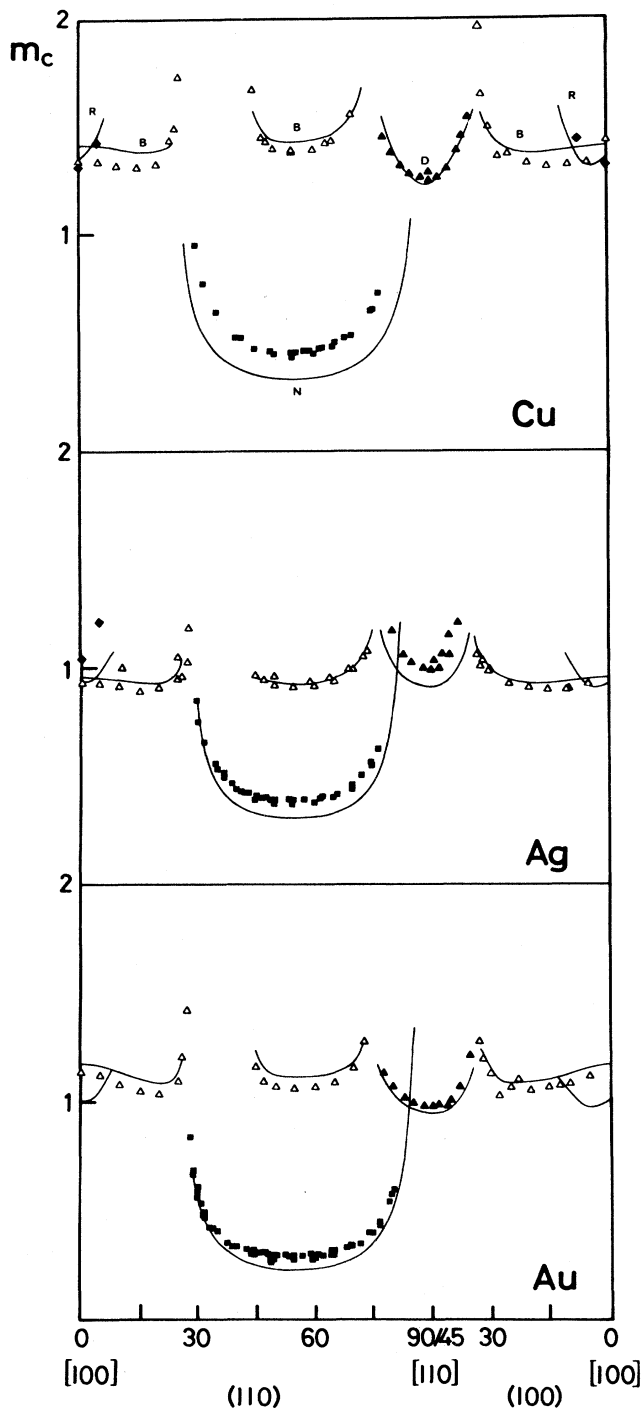


FIG. 3. The calculated (solid lines) and experimentally determined effective masses in free-electron mass units (see text for references) for the belly (open triangles), rosette (diamonds), dog-bone (solid triangles), and neck orbits (solid squares) as a function of magnetic field direction in the symmetry planes in copper, silver, and gold. In the upper panel we denote the different orbits with B (belly), D (dog bone), R (rosette), and N (neck). This notation covers all three studied systems.

ing in an electron-phonon interaction parameter of $\lambda=0.34$ for copper and $\lambda=0.20$ for silver and gold, when comparing the calculated values to those from Lengeler *et al.*¹⁴

The calculated g_c factors are presented in Figs. 4(a), 4(b), and 4(c) for copper, silver, and gold, respectively, together with experimental values from dHvA measurements. As for the effective-mass data no distinction is made between different references. The g_c^* factors were taken from Refs. 2, 17, and 18 for copper, Refs. 2 and 18

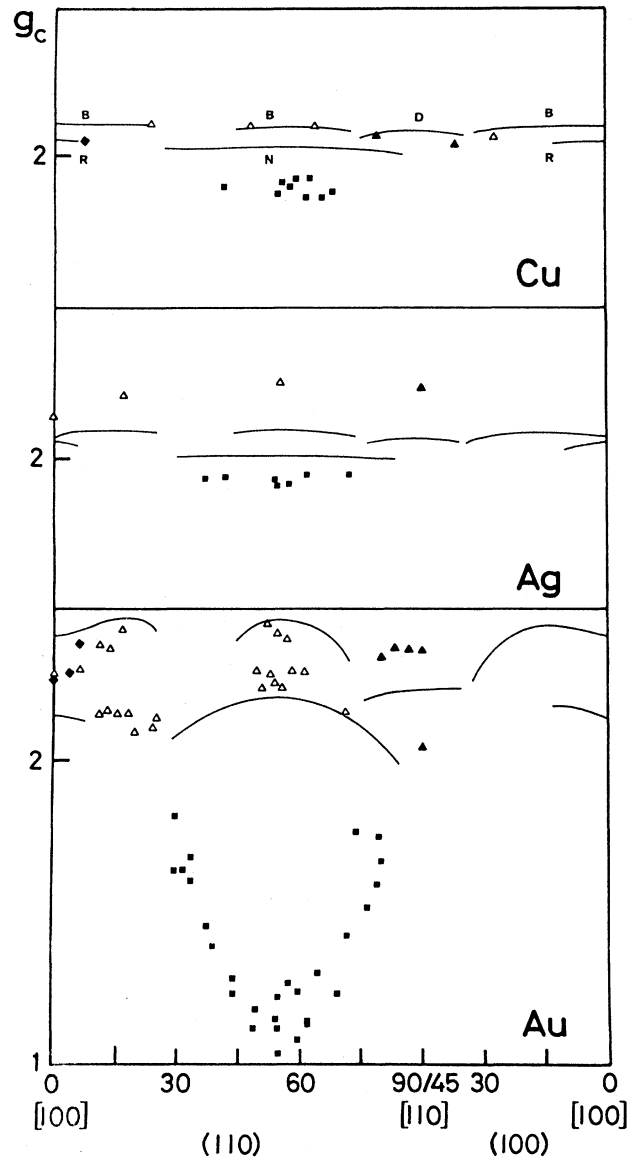


FIG. 4. The calculated (solid lines) and experimentally determined cyclotron-orbit g factors (see text for references) for the belly (open triangles), rosette (diamonds), dog-bone (solid triangles), and neck orbits (solid squares) as a function of magnetic field direction in the symmetry planes in copper, silver, and gold. In the upper panel we denote the different orbits with B (belly), D (dog bone), R (rosette), and N (neck). This notation covers all three studied systems.

for silver, and Refs. 2, 3, and 18–20 for gold. The calculations show that the g_c factors for copper and silver are similar, isotropic, and have small differences between different orbits while for gold the g_c factors exhibit a large anisotropy and have large differences between different cyclotron orbits. For all three metals the largest values are found on the belly orbit and the smallest on the neck orbit. In gold the belly orbit and the neck orbit have the largest anisotropy and both orbits show a maximum at [111] while a minimum is reached at [100] for the belly orbit. With increasing angle out from [100] a maximum is reached both in the (110) and (100) planes at approximately 20° which is followed by a sharp decrease in the (100) plane. For the rosette in gold the g_c factor decreases in value in the (110) plane while it increases in the (100) plane with increasing angle from [100]. Except for the neck orbit, the calculations are in good agreement with the experimentally determined values indicating that electron-phonon interaction and electron-electron exchange interaction are small for the belly, rosette, and dog-bone orbits in the noble metals. However, there is a scatter in the experimental data which is especially observable for the belly orbit in gold. This is mainly due to differences in the determined effective masses between different authors and to difficulties in determining the curvature factor which has to be calculated when the absolute amplitude method is applied. The curvature factor in the noble metals has been discussed in detail by Bibby *et al.*²¹ For the neck orbit in copper and silver the calculated g_c factors at [111] are 2.03 and 2.01, respectively, and a mean value for the g_c^* factors is 1.92 for both metals. Using Eq. (3) and the values for the electron-phonon parameter this results in a cyclotron Stoner enhancement of $S_c = 1.27$ and 1.15 for copper and silver, respectively. In gold $g_c = 2.20$ at [111] for the neck orbit and reducing this value with the electron-phonon interaction results in a value of 1.85 which is much higher than the experimental mean value of $g_c^* = 1.13$ at [111]. Furthermore, the variation with angle is different since the calculations show a maximum at [111] while for the experimental values derived from dHvA measurements a pronounced minimum is reached at [111].

IV. DISCUSSION AND CONCLUSIONS

It is interesting to compare this study with an independent but similar calculation using the linear muffin-tin orbitals (LMTO) method performed by Grechnev *et al.*²² The main differences between their work and this work is that Grechnev *et al.* have used correction structure constants and f orbitals and that the applied magnetic field was included in the self-consistent field calculation of the potential parameters. The difference in the resulting g_c at the symmetry directions for the same orbits is smaller than 2% compared to this work, which leads to the conclusion that the above-mentioned corrections are of minor importance.

The large discrepancy between theory and experiment of the neck orbit in gold has to be clarified further. The experimental results are based on two SSZ's on the fundamental harmonic and two SSZ's on the second harmonic

(see, e.g., Randles² and Crabtree *et al.*³) together with infinite field phase measurements by Coleridge and Templeton¹¹ which show that $\cos(\pi R) > 0$ at [111] for the neck orbit in gold. Thus, the next possible choice of the integer n besides $n=0$ which leads to the g_c^* factors presented in Fig. 4(c), gives a variation of g_c^* from 5.0 at 80.3° up to 13.4 at [111] (using the masses given in Ref. 3) and using Eq. (3), $S_c/(1+\lambda)$ varies correspondingly from 2.4 to 6.1. Such high values of g_c^* are not likely even though the contribution from the neck orbit to the total density of states must be small due to its small effective mass and therefore its g_c factors may deviate from the bulk value. On the other hand, when comparing the calculated values to the experimental results for the neck orbit presented in Fig. 4(c), $S_c/(1+\lambda)$ varies from 0.81 at 80.3° to 0.52 at [111], and using the m_c^* values from Ref. 3, $1+\lambda = 1.15$, this leads to the impossible situation that $S_c < 1$. The most probable reason for the discrepancy is therefore that the form of the operator used in the calculations for the spin-orbit coupling does not give a complete description, and it is thus clear that further studies are needed to explain the difference between theory and experiment on the neck orbit in gold.

The results presented in Fig. 4 also show that further experimental studies in the noble metals on the different orbits are needed in order to be able to make qualified comparisons between theory and experiment. Especially there are very few measurements performed in silver and in the (100) plane in all three metals. These calculations also show that it would be interesting to make a thorough study of the g_c^* factor in gold in the (110) and (100) plane besides the neck orbit since a large anisotropy is predicted by theory.

To summarize, these calculations clearly indicate that the anisotropy and deviation from the free-electron g value to a large extent can be explained by spin-orbit interaction. It is also shown that the g_c factors in copper and silver are isotropic with small differences in value between different orbits while the opposite seems to be true for gold, namely a large anisotropy, especially for the belly orbit, and a large difference in value between different orbits are found. Excluding the neck orbit, the calculations are in agreement with g_c^* factors determined from dHvA measurements indicating that for these orbits the electron-phonon interaction and electron-electron exchange enhancement are small. For the neck orbit in copper and silver the difference between theory and experiment can be explained by an electron-phonon mass enhancement of 1.34 and 1.20, respectively, and a cyclotron Stoner parameter of 1.27 and 1.15. Further studies are needed for the neck orbit in gold. The importance of further experimental studies of the g_c^* factor in the noble metals is also pointed out.

ACKNOWLEDGMENTS

Dr. Martin Lee is gratefully acknowledged for sending us a copy of his work prior to publication, and Dr. Johan Krause and Dr. Siri Kurland are acknowledged for fruitful discussions. This work has been supported by the Swedish Natural Science Research Council and The Bank of Sweden Tercentenary Foundation.

- ¹L. R. Windmiller and J. B. Ketterson, *Phys. Rev. Lett.* **21**, 1076 (1968).
- ²D. L. Randles, *Proc. R. Soc. London, Ser. A* **331**, 85 (1972).
- ³G. W. Crabtree, L. R. Windmiller, and J. B. Ketterson, *J. Low Temp. Phys.* **20**, 655 (1975).
- ⁴L. Nordborg, P. Gustafsson, H. Ohlsen, and S. P. Hornfeldt, *Phys. Rev. B* **31**, 3378 (1985).
- ⁵I. M. Lifshitz and A. M. Kosevich, *Zh. Eksp. Teor. Fiz.* **29**, 730 (1955) [*Sov. Phys.—JETP* **2**, 636 (1956)].
- ⁶S. Engelsberg and G. Simpson, *Phys. Rev. B* **2**, 1657 (1970).
- ⁷H. Ohlsen and J. L. Calais, *Phys. Rev. B* **35**, 7914 (1987).
- ⁸H. L. Skriver, *The LMTO Method* (Springer-Verlag, Berlin, 1984); O. K. Andersen, *Phys. Rev. B* **12**, 3060 (1975).
- ⁹B. R. A. Nijboer and F. W. de Wette, *Physica* **23**, 309 (1957).
- ¹⁰P. M. Holtham, *Can. J. Phys.* **51**, 368 (1973).
- ¹¹P. T. Coleridge and I. M. Templeton, *J. Phys. F* **2**, 643 (1972).
- ¹²D. Shoenberg and J. Vanderkooy, *J. Low Temp. Phys.* **2**, 483 (1970).
- ¹³P. T. Coleridge and B. R. Watts, *Can. J. Phys.* **49**, 2379 (1971).
- ¹⁴B. Lengeler, W. R. Wampler, R. R. Bourassa, K. Mika, K. Wingerath, and W. Uelhoff, *Phys. Rev. B* **15**, 5493 (1977).
- ¹⁵A. S. Joseph and A. C. Thorsen, *Phys. Rev.* **138**, A1159 (1965).
- ¹⁶A. S. Joseph, A. C. Thorsen, and F. A. Blum, *Phys. Rev.* **140**, A2046 (1965).
- ¹⁷P. T. Coleridge, G. B. Scott, and I. M. Templeton, *Can. J. Phys.* **50**, 1999 (1972).
- ¹⁸W. M. Bibby and D. Shoenberg, *J. Low Temp. Phys.* **34**, 659 (1979).
- ¹⁹H. Alles, R. J. Higgins, and D. H. Lowndes, *Phys. Rev. B* **12**, 1304 (1975).
- ²⁰G. W. Crabtree, L. R. Windmiller, and J. B. Ketterson, *J. Low Temp. Phys.* **26**, 755 (1977).
- ²¹W. M. Bibby, P. T. Coleridge, N. S. Cooper, C. M. M. Nex, and D. Shoenberg, *J. Low Temp. Phys.* **34**, 681 (1979).
- ²²G. E. Grechnev, N. V. Savchenko, I. V. Svechkarev, M. J. G. Lee, and J. M. Perz, *Phys. Rev. B* **39**, 9865 (1989).